Materials Science-Poland, Vol. 25, No. 1, 2007

Experimental challenges for approaching local strain determination in silicon by nano-Raman spectroscopy*

L. ZHU[1,2], J. ATESANG[1, 3], P. DUDEK[1, 4], M. HECKER[1**], J. RINDERKNECHT[1], Y. RITZ[1], H. GEISLER[1], U. HERR[2], R. GEER[3], E. ZSCHECH[1]

[1]AMD Saxony LLC & Co. KG, Materials Analysis Department, Wilschdorfer Landstrasse 101, D-01109 Dresden, Germany

[2] University of Ulm, Materials Department, Albert-Einstein-Allee 47, D-89081 Ulm, Germany

[3] University at Albany-SUNY, College of Nanoscience and Engineering, NanoFab 300 South, 255 Fuller Rd. Albany NY 12203, USA

[4] Wrocław University of Technology, Faculty of Microsystem Electronics and Photonics, ul. Janiszewskiego 11/17, 50-372 Wroclaw, Poland

Raman intensity enhancement induced by nanoprobes (metal particles and metallised tips) approached to a strained silicon sample surface is reported. With silver nanoparticles deposited onto a silicon surface, high enhancements in the vicinity of particles were observed. Furthermore, metallised tips were scanned inside the spot of the laser used for Raman measurements. Both silver-coated and pure silver tips, mounted onto a tuning fork, indicated high Raman signal enhancement for optimised tip position within the laser spot. Atomic force microscopy was performed on a structured sample to investigate the stability of these tips. Focused ion beam was utilized to refine and to re-sharpen pure silver tips after the measurements. Complementary measurements were performed using pure tungsten tips. Due to the high hardness of W wires, a special pre-etching technique was applied in this case.

Key words: *Raman scattering; strained silicon; Ag particles; tip enhanced Raman spectroscopy*

1. Introduction

Increasing product performance and achieving a continuous cost reduction per function have been for several decades the driving forces for scaling down CMOS device dimensions. Traditional scaling of the device structures alone, however, will

---

* Presented at the joint events 1st Workshop "Synthesis and Analysis of Nanomaterials and Nanostructures" and 3rd Czech-Silesian-Saxony Mechanics Colloquium, Wrocław, Poland, 21–22 November, 2005.

** Corresponding author, e-mail: michael.hecker@amd.com

not be sufficient to meet future performance goals. New materials and "non-classical" devices are developed and implemented, resulting in new challenges for the device metrology. Strain engineering has become an important tool; for example, strained silicon has been used to affect the electronic band structure and to increase charge carrier mobility in the channel region of MOSFET devices. New analytical techniques for high-resolution strain measurement at transistor cross-sections and new metrology strategies to monitor non-destructively strain variations are needed to optimise and control the variety of processes, including those for strained silicon substrates and for utilizing process-induced local strain.

The potential for measuring local strain in the transistor channel with high spatial resolution is limited to a few techniques. Techniques based on transmission electron microscopy (TEM) such as convergent beam electron diffraction (CBED), nanobeam diffraction (NBD), and high-resolution TEM (HRTEM) [1, 2], as well as nano-Raman spectroscopy [3, 4] are currently being evaluated for their applicability to measure strain with a spatial resolution in the 10 nm range. In particular, approaches based on Raman spectroscopy are promising due to fewer preparation issues and higher sample throughput. They have been proven to be well suited to strained silicon problems on the μm scale [5].

Since the first report of Anastassakis et al. [6] related to the effect of strain on the Raman peak position, Raman spectroscopy has been widely applied as a stress sensor. The Raman signal, however, is intrinsically weak (less than 1 in 10^7 photons), and its spatial resolution is limited by the optical diffraction limit. This resolution limit can be overcome by scanning near field microscopy (SNOM) utilizing an apertured fibre tip, however the intensity issue becomes even worse [7]. After the discovery of significantly enhanced Raman signals of pyridine molecules due to rough silver electrodes by Fleischmann et al. [8], Jeanmaire and van Duyne found that the differential Raman cross section of molecules in liquid or gaseous phases receives a huge enhancement upon adsorption on rough noble metal surfaces [9]. The so-called surface enhanced Raman spectroscopy (SERS) can be applied not only to bulk metallic materials, but also to metal nanoparticles, and even evaporated thin silver films [10]. The limitation of the nanoparticle approach is that the particles should be deposited exactly in the region of interest. As an alternative, an apertureless approach is to utilize metal tips, employing the tip enhanced Raman spectroscopy (TERS) effect, which can increase the Raman intensity by several orders of magnitude [11, 12]. In this case, the signal enhancement is due to the enhancement of the electromagnetic field in the vicinity of a sharply pointed tip, resulting from the excitation of surface plasmons by the incident laser beam. Metallic tips can be made of or coated with certain metals (e.g. Ag, Au), or nanoparticles can be attached to the tip. It has been reported that parallel silicon lines with 300 nm line-widths, separated by 380 nm SiO_2 lines, can be resolved utilizing a metal-coated fibre tip [13]. The near field approach, TERS, seems to allow a spatial resolution of the Raman signal well below 100 nm to be reached.

In this paper, experimental challenges are described for obtaining the silver-based SERS/TERS effect using nanoparticles and shape-optimised pure silver and silver-coated tips.

2. Experimental

2.1. Measurement set-up

The measurement system consists of a Renishaw spectrometer with a confocal microscope for Raman measurements [14], combined with a Nanonics Atomic Force Microscopy (AFM) system for navigating a metallic tip close to the sample surface inside the laser spot. The integration of these two systems is controlled by dynamic data exchange software allowing the system to acquire simultaneously AFM data and Raman spectra.

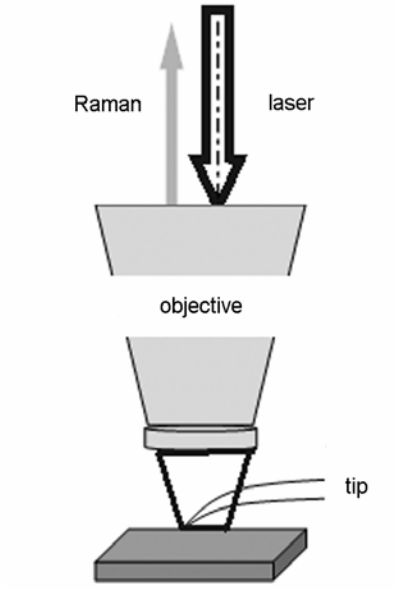

Fig. 1. Schematic set-up diagram of tip enhanced Raman scattering. The tip was positioned inside the laser spot between the objective lens and the sample surface. The Raman light is backscattered through the same objective lens to the grating and detector

For the AFM part, a cantilevered tip, fixed to a tuning fork, is used (Fig. 1). The tip can be controlled both when it is approached to the surface below the objective lens ("in feedback", distance to surface being several nanometers) and when it is "retracted" (distance to surface several μm).

The Raman system is equipped with a Leica microscope and a motorized stage placed in an enclosure chamber. The 50× objective (numerical aperture 0.45, working distance 1 cm) used in our experiments focuses the laser to a spot size of about 3 μm and has a convergence angle of 26°. This facilitates adequate access of the laser to the tip below the objective. The collected signal is detected by a charge coupled device (CCD) cooled by a Peltier cooling system. The spectrometer uses several gratings, from which one can be selected for spectra acquisition for different laser wavelengths. For the measurements presented here, Ar-ion lasers with 488 nm and 514 nm wavelengths were used.

2.2. Tip preparation

Tip preparation is crucial for TERS measurements, because the radius, shape, and material of the tip determine the enhancement factor and spatial resolution. To obtain a highly localized field enhancement, a tip with a small diameter and sharp end should be used for TERS. Pure metallic tips were prepared using electrochemical etching of silver and tungsten wires. This preparation technique provides good quality tips in a reproducible and reliable way [15, 16]. The principal set-up for etching both kinds of tips is based on a commonly used configuration [17], as shown in Fig. 2. For our experiments, an aqueous solution with approximately 60% perchloric acid and ethanol (1:2 or 1:3), and an applied voltage from 1.5 V to 1.8 V, were selected for silver tip etching [18]. A diluted KOH solution (3 mol/dm^3: 56 g KOH in 333 ml of water) and an applied voltage between 1.8 V and 2.1 V were chosen for tungsten tip etching [19].

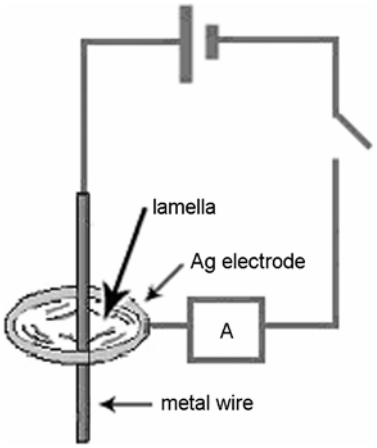

Fig. 2. Schematic diagram of electrochemical etching. The metal wire (anode) is situated in the middle of the lamella inside a silver ring that acts as a cathode during etching

Since a tungsten wire is much harder and stiffer than a silver one, it is much more difficult to cut the etched tungsten tips to a proper length with a wire cutter. Therefore, an additional process called "pre-etching" was developed. Prior to the actual tungsten tip etching, the tungsten wire was etched at a specific position to generate a "pre-determined breaking point". Subsequently, the tungsten wire was finally etched and separated. The scanning electron microscopy (SEM) picture of a tungsten tip after "pre-etching" (Fig. 3) clearly shows that the thinner part originating from the "pre-etch" can be cut later in a well-defined way. Furthermore, the length of the tip after the final cut can also be controlled by the position of the "pre-etch".

The mounting of the tips to the tuning fork (Fig. 4) was done in such a way that the total mass of tip and glue added onto the tuning fork was as small as possible. This method should minimize the damping of the tuning fork resonance frequency and, consequently, enables a high sensitivity to be maintained during feedback. Epoxy (Epo-Tek 375) was used to glue the tip to the tuning fork. The epoxy was cured at 90 °C for 90 minutes. It showed excellent adhesion between the tip and tuning fork.

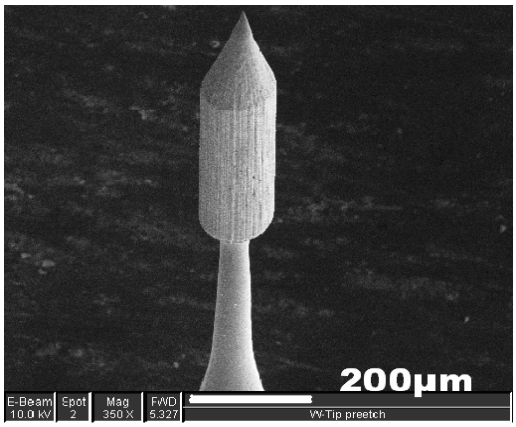

Fig. 3. SEM image of a tungsten tip after a "pre-etch" treating for local thinning below the tip apex

Fig. 4. Schematic picture showing a tip mounted to a normal tuning fork

By using a 45° mounting angle, a good compromise to minimize the laser and Raman light shadowing and to maximize the enhancement effect was achieved.

2.3. Preparation by FIB

The Focused Ion Beam (FIB) technique [20] was used combined with micromanipulators for target cross-section preparation of samples subsequently imaged by

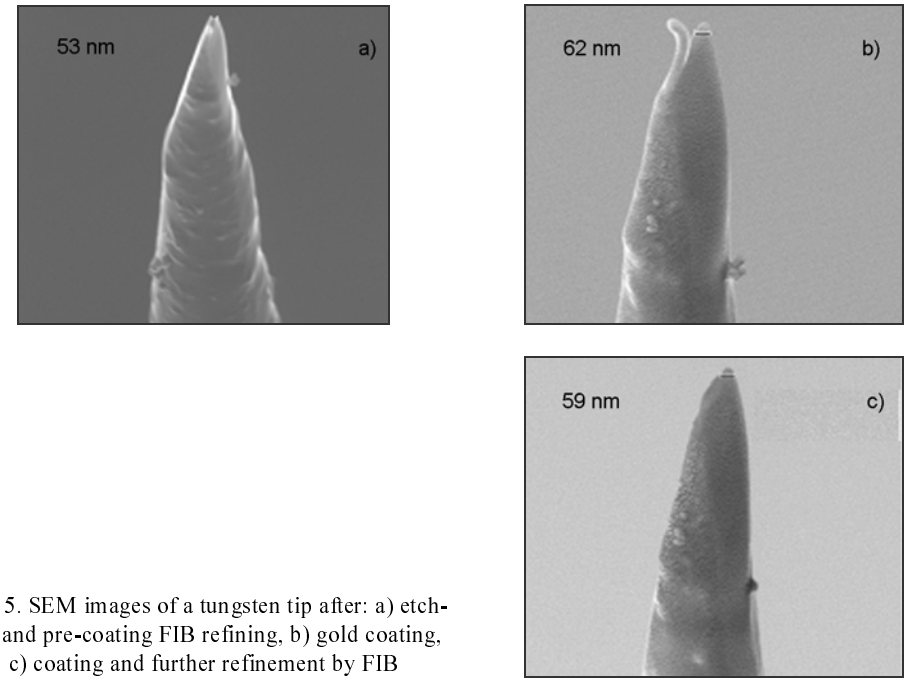

Fig. 5. SEM images of a tungsten tip after: a) etching and pre-coating FIB refining, b) gold coating, c) coating and further refinement by FIB

lamella can be prepared by the lift-out technique directly from the region of interest of the sample, which is lifted using a needle manipulator [21, 22]. This method is also an attractive technique for fabrication and modification of metallic nanostructures. In our application, the FIB technique was used to refine or re-sharpen metallised tips. A FEI dual-beam FIB (Strata 235), with a built-in needle Omniprobe manipulator, was applied to modify the tips. For example, after etching, a pure W tip was refined and milled by FIB as shown in Fig. 5a. After subsequent gold coating, a defect in the gold capping was found (Fig. 5b). Finally, this gold coated W tip was re-sharpened to achieve a diameter of about 60 nm (Fig. 5c). This refinement technique is limited to a maximum rotation of 66° (from –12° to 54°) of the tip itself, which determines the type of tips that can be prepared or modified using the FIB technique without readjusting the tips.

3. Results of measurement and discussion

Bulk Si samples are often used for TERS measurement [13], whereas in our application a special film stack was utilized, consisting of a 70 nm strained Si layer on top of 150 nm thick SiO_2 and the Si substrate. Since the penetration depth of 488 nm laser light in Si is about 500 nm, a two-peak spectrum was obtained for the first-order Si–Si phonon modes, which can be well fitted with two Lorentzian curves. The lower frequency at about 516 cm^{-1} represents a strained Si peak, and the peak appearing at 521 cm^{-1} corresponds to the Si bulk peak. Monitoring the intensity ratio between these two peaks allows us to distinguish between conventional (far field) Raman measurements, shadowing effects, and enhancement effects. Moreover, information regarding the penetration depth related to the near field can be derived from measuring layer stacks.

3.1. Enhanced Raman scattering intensity close to silver particles

Nanoparticles of noble metals such as Ag or Au deposited onto the surface of a Raman active sample potentially lead to a Raman signal enhancement caused by SERS. The described particles were obtained from a solution containing Ag nanoparticles with sizes ranging from 20 nm to 300 nm. A droplet of a mixture of this solution and deionised water (volume ratio 1:4) was deposited on the sample surface with a pipette and evaporated at room temperature. SEM was used to characterize the deposited silver as shown in Fig. 6a. Subsequently, a Raman mapping with a step size of 0.1 μm in both x and y directions utilizing the 488 nm laser was conducted. The mapped intensity at wavenumber 516 cm^{-1} (Fig. 6b) corresponding to the position of the strained Si film peak exhibits high enhancement effects. A comparison with the spectrum taken from the bottom part of the Raman mapping and far from the particles reveals an enhancement of the strained Si peak intensity by around 75% without sig-

nificant change of the Si bulk peak intensity and background signal (Fig. 7). This example of the strong amplification of the evanescent near field close to a nanoparticle reflects the high depth resolution that can be achieved utilizing the SERS effect compared to the far field signal which is related to the normal penetration depth of the incident laser.

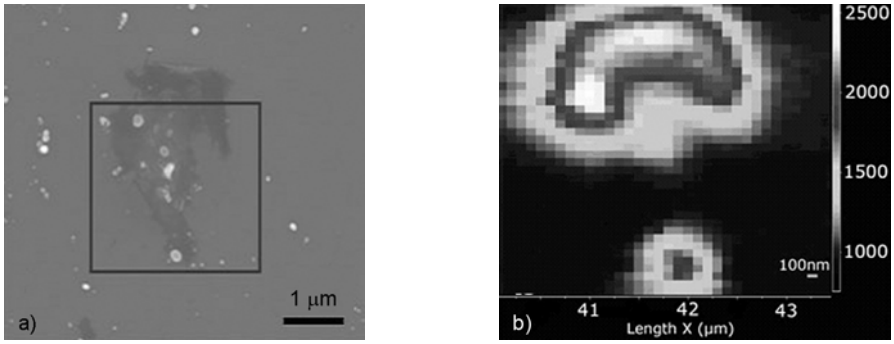

Fig. 6. SEM image with the size of 6.5×6.5 µm^2 (a), and Raman mapping utilizing the 488 nm laser (b) with the size of 3.5×3.5 µm^2. The grey scale indicates the intensity of the strained silicon film peak at the wavenumber of 516 cm^{-1}

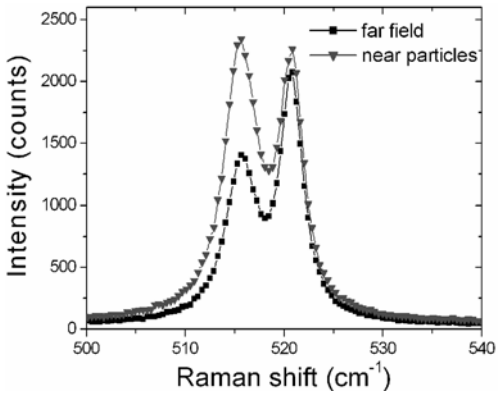

Fig. 7. Spectra obtained at a sample position far from particles (far field) and close to particles, utilizing the 488 nm laser

From the SEM picture shown in Fig. 6a and the Raman map in Fig. 6b taken at the same area it is possible to correlate the bottom part of the Raman map to the single particle shown in the SEM picture. Due to the selected deposition procedure, there are also regions such as those in the top parts of both pictures, where no exact correlation was obtained because of high particle density.

3.2. Tip enhanced Raman scattering with silver tips

As discussed in Section 2, pure silver tips were produced by an electrochemical etching method. The Ag tips, properly etched and mounted to a tuning fork, were carefully approached to the sample surface by the AFM table located below the objective lens and then slightly retracted (to a distance of several hundred nm). Raman

spectra of the sample below the tip as shown in Fig. 8 were measured under this condition and compared with a measurement obtained with the tip far away from the laser spot ("far field" measurement).

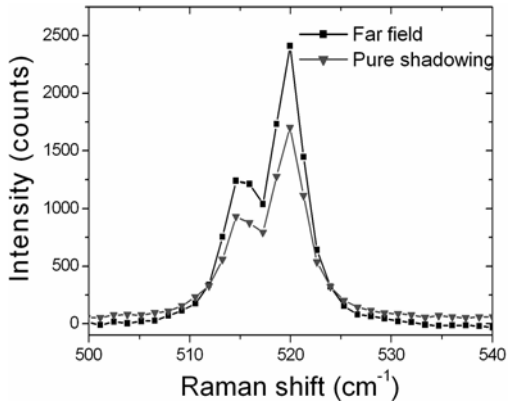

Fig. 8. Spectra taken without the tip (far field) and with the tip slightly retracted, showing the shadowing effect of the tip. The laser wavelength of 488 nm was used

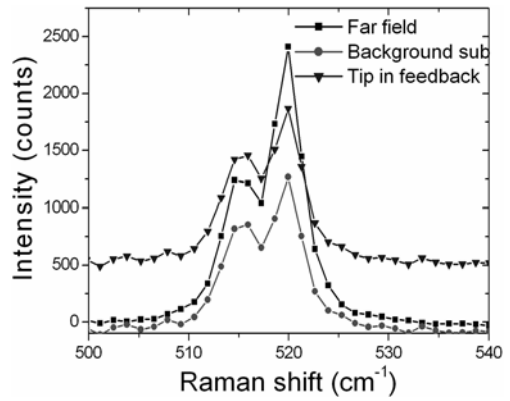

Fig. 9. Spectra obtained without the tip (far field), with the tip in feedback, and background subtracted, utilizing the 488 nm laser

After curve fitting, the intensity ratio between both peaks was found to be unchanged for these two spectra. Furthermore, both peak intensities are lower for the tip in feedback, indicating a pure shadowing effect. After this measurement, the tip was approached to the sample surface again and navigated inside the laser beam to obtain enhanced intensities. Enhancement effects as shown in Fig. 9 were obtained only in a small *xy* range inside the laser beam. A high background, which might arise from a contamination on the tip surface, was subtracted for curve fitting. After this subtraction, no increment for the strained Si peak intensity due to the approached tip was obtained. This result may be related to the high background and strong shadowing effect by the tip. However, an enhancement effect can be derived from the change of the intensity ratio between the Si bulk peak and the strained Si peak. According to Fig. 9, this ratio changed from 2.1 for the far field measurement to 1.4 for the tip in feedback. Possibly, an additional cleaning procedure of the silver tips could reduce the background signal.

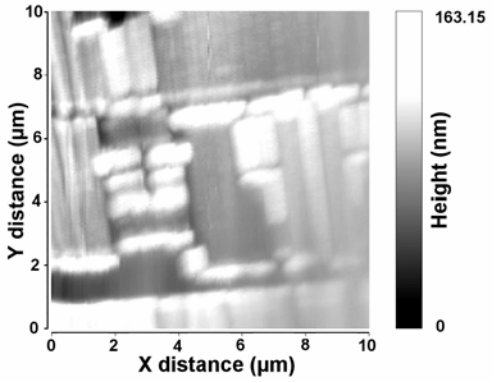

Fig. 10. AFM mapping graph of a structured sample using a silver tip

AFM scanning of the region of interest is necessary to characterize laterally structured samples by such tips and to correlate surface morphology to measured Raman features. Figure 10 shows an example obtained with the Ag tip used in Fig. 9, which demonstrates the principal possibility of obtaining AFM scans by these tips. After scanning, however, most of the self-prepared silver tips were bent, apparently because silver is very ductile compared to other AFM tip materials. One possibility to overcome this problem is to use FIB preparation to re-sharpen the bent tips. With FIB, tips of good quality with the diameter of approximately 40 nm were obtained. Another possibility to combine AFM mappings and Raman enhancement experiments is to use W tips coated with Ag or Au. FIB was used to sharpen and refine tips before and after coating, too. A third way, utilizing metal coated quartz tips, is discussed below.

3.3. TERS measurements with silver coated quartz tips

As observed for pure Ag tips, Raman enhancement effects are obtained only for a certain position of the tip inside the laser spot. For a more systematic study, measurements were performed by *xy* scanning the tip in the feedback mode inside the 514 nm laser spot, with fixed positions of the laser spot and sample. During such AFM scans, Raman spectra were acquired at specific positions, thus yielding Raman maps for tip positions inside the whole defined area. After curve fitting, the Raman intensities related to the Si bulk peak and to the strained Si peak are shown separately in Fig. 11. The left Raman mapping showing the Si bulk peak intensity clearly indicates a gradual shadowing effect. During tip scanning, an increasing part of the tip inhibits laser light from illuminating the sample surface, leading to a decrement of the overall bulk Raman signal. Raman mapping of the strained Si peak intensity shows that there is a large enhancement without increased background inside the area where shadowing effects for the Si bulk peak intensity occur. As a reference, a spectrum was also recorded with the tip outside the laser spot. Both spectra in Fig. 12 were fitted using the Lorentzian function. The enhancement for the strained Si peak is 48%, and the decrement of the Si bulk peak intensity is about 7% as compared to the “far field”

spectrum. This result should be referred to a local field enhancement close to the tip and restricted to the strained Si layer, not propagating into the Si bulk.

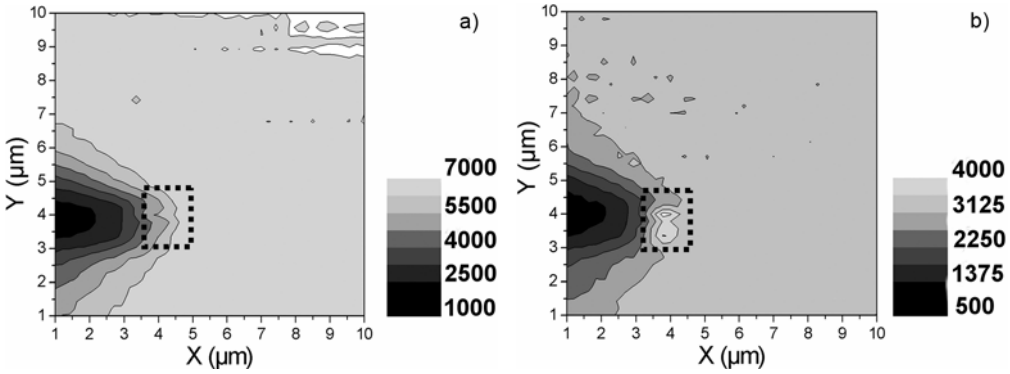

Fig. 11. Raman mapping of: a) Si bulk intensity (521 cm^{-1}) utilizing a 514 nm laser, b) strained Si layer intensity (516 cm^{-1}) utilizing a 514 nm laser. The sizes of both mappings are 10×10 μm^2

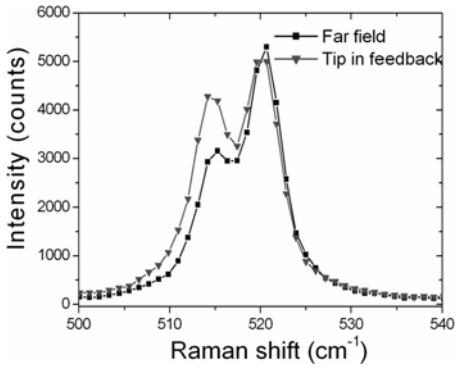

Fig. 12. Raman spectra obtained from tip scanning utilizing a 514 nm laser. "far field" spectrum denotes a spectrum taken with the tip outside the laser spot

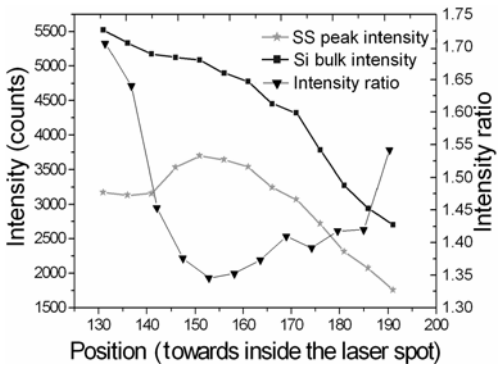

Fig. 13. Curves of strained Si peak intensity I_{sSi}, Si bulk peak intensity I_{Si} and intensity ratio I_{Si}/I_{sSi} for the tip scanning the laser spot utilizing a 514 nm laser

The enhancement was verified by navigating the tip manually inside the 514 nm laser spot. First, for the tip positioned outside the laser spot, a spectrum was acquired. Subsequently, the tip was moved inside the laser spot with a step size of 125 nm. The Si bulk peak intensity curve shown in Fig. 13, with the tip successively approaching the laser spot, indicates that the shadowing effect increases while moving the tip towards the centre of laser spot. At specific positions within the spot, the strained Si peak intensity is increased. This observation can be seen more clearly in the intensity ratio curve (Fig. 13). The spatial extension of the region with low intensity ratio, i.e. an enhancement of the strained Si layer intensity, was found to be sensitive to the tip properties. As a consequence, in order to avoid strong shadowing effects and achieve high enhancement at the same time, the tip position should be near the edge of the laser spot.

In order to confirm the TERS effect from these tips, a "two-point" mapping was performed, i.e. two spectra were taken at each point, one for the tip in feedback and one for the tip retracted by about 8 μm from the sample surface. Furthermore, the difference between these two spectra was calculated for every scanning point. The mapping of the difference spectrum at the wavenumber 516 cm^{-1} (Fig. 14) clearly shows that besides the "island", i.e. the enhancement area, all other regions show a small or almost no difference signal.

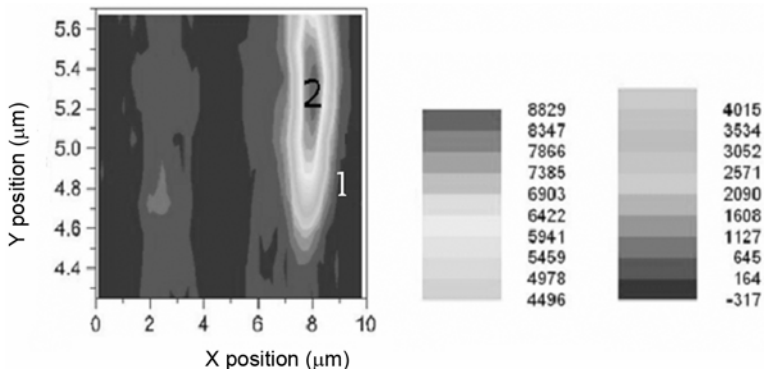

Fig. 14. Raman mapping of the difference spectrum at 516 cm^{-1} utilizing a 514 nm laser

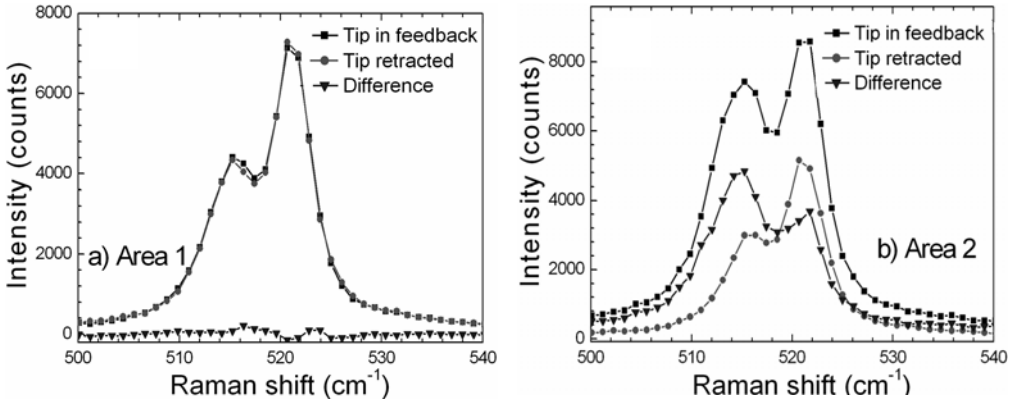

Fig. 15. Spectra obtained from areas 1 and 2 in Fig. 14, corresponding to the tip being retracted (about 8 μm), the tip in feedback, and the difference between the two spectra, utilizing a 514 nm laser

In area 1 of Fig. 14, there is almost no difference between the spectra taken with the tip in feedback and with a retracted tip (Fig. 15a), which means that the tip was totally outside the laser spot. Therefore the spectra taken inside area 1 can be regarded as "far field", i.e. spectra acquired without a tip or any influence of the tip. Within area 2, a high enhancement was achieved (Fig. 15b). Upon retraction, the tip moved towards the centre of the laser spot causing increased shadowing. Therefore, "far field" spectra obtained inside area 1 should be used for direct comparison with the

enhanced spectra acquired inside area 2, if the shadowing effect is not considered thoroughly. From curve fitting an enhancement for the strained Si peak intensity of 93% and a slight intensity increment for the Si bulk peak intensity of 8% was obtained. Note that inside the mapping shown in Fig. 14, the positions of area 1 and area 2 are rather close. Since area 1 is the area where the tip was outside the laser spot, in area 2 the tip should be close to the edge of the laser spot. This result confirms the proposed optimum tip position for highest enhancement. From the mapping data in Fig. 14, the size of the area in which high enhancement is achieved is about 500×500 nm^2.

4. Conclusions

To investigate the surface enhanced Raman scattering of strained silicon samples, both silver nanoparticles and metallised AFM tips were approached to the surface of a silicon layer stack. The top silicon layer was strained, enabling the enhancement effects close to the surface and in the bulk of the sample to be observed separately.

For silver nanoparticles deposited on the layer stack, a high enhancement of the strained Si intensity (~ 75%) was observed. The locations of the enhanced Raman signal were correlated to the particles using SEM. In contrast to the signal from the top layer about 70 nm thick, no significant enhancement of the Si bulk peak occurred.

Pure silver tips etched by an electrochemical method were mounted to an AFM tuning fork for measuring enhanced Raman signals. Clear enhancement effects were observed, and the potential of such tips for AFM scanning was proven. The use of such tips, however, is limited by bending effects occurring during AFM scanning. The possibility of re-sharpening bent tips by FIB was verified. An improvement of tip stability is expected for tungsten tips prepared by electrochemical etching, which can be coated by a SERS inducing metal film.

With silver coated quartz tips, Raman peak enhancement of the strained silicon film up to 50% was achieved by navigating the tip inside the laser spot and moving it to an optimised position. This was achieved by performing tip scans with the tip in feedback, and by "two-point" tip mappings, i.e. measurements of two Raman spectra at each point. These experiments indicate that the optimal tip position for highest enhancement is close to the edge of the laser spot.

The experiments performed with metallised tips are promising for achieving high local strain resolution in patterned Si structures by utilizing the described difference measurements ("two-point mappings") in TERS experiments. Further efforts are necessary to prevent the oxidization of the silver coating, and to achieve long-term stability of both the tip itself and enhancement effect.

Acknowledgements

The authors would like to thank Boleslaw Mazurek, Wrocław University of Technology (Poland) for providing the Ag particle solution, Petra Hofmann, AMD Saxony LLC & Co. KG (Germany) for SEM support, as well as Hartmut Prinz, also with AMD Saxony LLC & Co. KG, and Othmar Marti, University of Ulm (Germany) for their helpful discussions.

References

[1] MORNIROLI J.P., ALBAREDE P.H., JACOB D., [in:] E. Zschech, C. Whelan, T. Mikolajick (Eds.), *Materials for Information Technology*, Springer, London, 2005, p. 99.
[2] FORAN B., LIAN G., CLARK M.H., Future Fab. Intl. 20 (2006), 127.
[3] ATESANG J., GEER R.E., [in:] R.E. Geer, N. Meyendorf, G.Y. Baaklini, B. Michel (Eds.), SPIE Proc., 2005, p. 134.
[4] PRIKULIS J., MURTY K.V.G.K., OLIN H., KÄLL M., J. Microscopy, 210 (2003), 269.
[5] HECKER M., GEISLER H., Mater. Sci.-Poland, 25 (2007), 7.
[6] ANASTASSAKIS E., PINCZUK A., BURSTEIN E., POLLAK F.H., CARDONA M., Solid State Commun., 8 (1970), 133.
[7] LEWIS A., TAHA H., STRINKOVSKI A., MANEVITCH A., KHATCHATOURIANTS A., Nature Biotechn., 21 (2003), 11.
[8] FLEISCHMANN M., HENDRA P.J., MCQUILLAN A.J., Chem. Phys. Lett., 26 (1974), 163.
[9] JEANMAIRE D.L., VAN DUYNE R.P., J. Electroanal. Chem., 84 (1977), 1.
[10] HAYAZAWA N., MOTOHASHI M., SATIO Y., KAWATA S., Appl. Phys. Lett., 86 (2005), 263114.
[11] MEHTANI D., LEE N., HARTSCHUH R.D., KISLIUK A., FOSTER M.D., SOKOLOV A.P., MAGUIRE J.F., J. Raman Spectrosc., 36 (2005), 1068.
[12] PETTINGER B., REN B., PICARDI G., SCHUSTER R., ERTL G., Phys. Rev. Lett., 92 (2004), 096101.
[13] SUN W.X., SHEN Z.X., Mater. Phys. Mech., 4 (2001), 17.
[14] Available online at: http://www.renishaw.com/client/product/UKEnglish/PRD-1027.shtml
[15] GUISE O.L., AHNER J.W., JUNG M.C., GOUGHNOUR P.C., YATES J.T., Jr., Nano Lett., 2 (2002), 191.
[16] KLEIN M., SCHWITZGEBEL G., Rev. Sci. Instrum., 68 (1997), 3099.
[17] REN B., PICARDI G., Rev. Sci. Instrum., 75 (2004), 4.
[18] IWAMI M., UEHARA Y., USHIODA S., Rev. Sci. Instrum., 69 (1998), 4010.
[19] ITO T., BUEHLMANN P., UMEZAWA Y., Anal. Chem., 70 (1998), 255.
[20] GIANUZZI L.A., STEVIE F.A. (Eds.), *Introduction to Focused Ion Beams*, Springer, New York, 2004.
[21] ALTMANN F., Pract. Metallography, 40 (2003), 175.
[22] RITZ Y., STEGMANN H., ENGELMANN H.J., ZSCHECH E., Pract. Metallography, 41 (2004), 180.

Received 3 January 2006
Revised 28 May 2006